

An Hierarchical Markov Random Field Model for Bayesian Blind Image Separation

Feng SU

State Key Laboratory for Novel Software Technology
Nanjing University, Nanjing, 210093, P.R.China
suf@graphics.nju.edu.cn

Ali MOHAMMAD-DJAFARI

Laboratoire des Signaux et Systemes, UMR 8506 (CNRS-Supelec-UPS)
Supelec, 3 rue Joliot Curie, Gif-sur-Yvette, 91192, France
djafari@lss.supelec.fr

Abstract

In this paper we propose an hierarchical Markov random field (HMRF) model and the Bayesian estimation frame for separating noisy linear mixtures of images constituted by homogeneous patches. A latent Potts-Markov labeling field is introduced for each source image to enforce piecewise homogeneity of pixel values. Based on classification labels, the upper observable intensity field is modeled by the combination of Markovian smoothness of intensity inside a patch and conditional independence at the edges. The correlation between multiple color channels, which share the same common classification, is exploited to stabilize the separation process. All unknown quantities including the sources, labels, mixing coefficients and distribution hyperparameters are formulated in the Bayesian framework and estimated by MCMC simulation of their corresponding posterior laws. The performance of the proposed model is shown by experiment results on both synthetic and real images, along with some comparisons with the ICA approach.

1 Introduction

The separation or reconstruction of unknown source images from their observed mixtures is a fundamental task for a wide range of image processing problems. In its basic form, the problem can be stated as: given M observed images $\{X_i, i = 1, \dots, M\}$, we want to estimate the N original source images $\{X_i, i = 1, \dots, N\}$ on the basis of cer-

tain assumptions about the data generation model. Though the underlying mixing form (linear or nonlinear, instantaneous or convoluting) and the noise type usually can be assumed *a priori*, their parameters are not known in advance and to be estimated together with the sources, which constitutes a typical ill-posed problem. Due to its generality and representativity to practical observation processes, the described model is widely employed in many multi-source imaging problems [3, 6, 1, 2].

From the viewpoint of the signal processing field, unsupervised separation of images can be viewed as one particular type of *blind source separation* (BSS) problem, for which some general solutions such as Principal Components Analysis (PCA) and Independent Components Analysis (ICA) have been proposed. Based on seeking uncorrelatedness (PCA) or maximum mutual independency (ICA) between output components of an inverse linear transformation, these methods have shown their applicability and effectiveness in many blind image separation problems, sometimes with certain variations of the model assumption such as nonlinearity or convolution [5]. However, besides the cross-image independency, it's usually helpful or necessary to exploit the intrinsic constraints or structures within an image, rather than just taking image as random signal sequence, to regulate the essentially ill-posed separation task. For integration of these information, the Bayesian inference framework provides sufficient flexibility through hierarchical prior and causality modeling, which is usually lacked in basic ICA/PCA-based methods.

One commonly exploited characteristic for a large number of images is the Markovian property, that is, the local

spatial correlations among pixels (sites) within a limited range of the image surface. To numerous context-dependent variables of this form, Markov random field (MRF) theory provides a consistent estimation and inference model. By introducing additional interacting layers of MRF, more sophisticated models such as hidden or hierarchical MRF (HMRF) can be built to describe specific priori constraints encoded in the image. On the other hand, image features like smoothness or discontinuity can also be expressed by different forms of potential functions in the Gibbs distribution of MRF.

Both HMRF model and Bayesian approach have been extensively used in enhancement, restoration, segmentation and other classical image processing problems. In Bayesian blind image separation, however, relatively few models have been proposed and even fewer addressed separation of multi-channel image data. The reference in [8] describes one model, which models the monochromatic source by a Potts-MRF directly on the pixel intensity (no latent labeling), but with an explicit edge term encoded in the potential corresponding to the discontinuity at object borders. Though satisfactory results were reported by existing methods on monochromatic data, the availability and appropriate exploitation of multi-channel information are supposed to increase the separation performance and stability.

In this paper, we propose an hierarchical Markov random field model and the Bayesian estimation frame for separating noisy linear mixtures of multichromatic images. We assume the source images are comprised of piecewise homogeneous patches and employ two-layer MRF model to account for the smoothness inside a patch and conditional independence at the edges, as well as the implicit correlation between different color channels. In section 2, we describe the HMRF used to model source images. Then, we give probabilistic characterization of the BSS problem in section 3. In section 4, the Bayesian estimation framework for model parameters is described. At the end, experiment results of the proposed algorithm are presented with some comparisons between different approaches.

2 Hierarchical Markov random field model

Unlike most PCA/ICA based methods that treat image as a sequence of temporal signals without further finegrained subsection, we model every source image with an hierarchical Markov random field for its convenience in describing the image structure and the underlying generation model. As illustrated in Fig.1, this model consists of two layers of Markovian random processes - the *label field* and the *intensity field*, interconnected between each pair of corresponding sites.

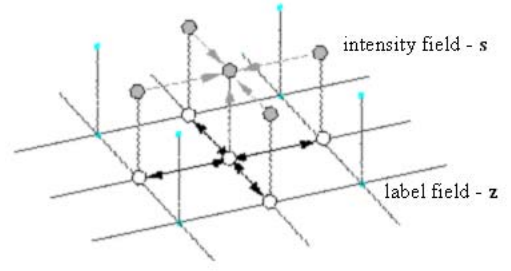


Figure 1. Hierarchical Markov random field model.

2.1 Label field

The label field is composed of the latent classification labels for every pixel in image. Supposing the content of j th source image can be divided into K_j classes, the corresponding label field is represented by a set of discrete variable $\mathbf{z}_j = \{z_j(r), r \in \mathcal{R}\}$ (\mathcal{R} for all pixel sites), which are valued in $\{1, \dots, K_j\}$. Different source images can contain varied number of pixel classes, which is usually task-depending, and in the simplest case, we may choose $K_j = 2$ to distinguish between foreground object and the background.

In this work, we define one pixel class as a distinct yet internally uniform set of color values that owned by some spatially connected pixels. By this definition, the label field is inherently with the local homogeneity property and thereby can be naturally modeled by the Potts-Markov random field prior distribution:

$$p(\mathbf{z}_j) \propto \exp \left[\beta_j \sum_{r \in \mathcal{R}} \sum_{r' \in \mathcal{V}(r)} \delta(z_j(r) - z_j(r')) \right] \quad (1)$$

where, $\mathcal{V}(r)$ denotes the neighbor sites of the site r , and the parameter β reflects the degree of smoothing interactions between pixels and controls the mean size of homogeneous area.

2.2 Intensity field

The intensity field is comprised of observable pixel values at every site of the image. For one pixel $s_j(r)$ at site r of j th image, its intensity distribution is conditioned (maybe partially) on the the class label $z_j(r)$ that the pixel has. Given the label, we assume the distribution $p(s_j(r)|z_j(r))$ is Gaussian, so that the distribution $p(s_j(r))$ is a mixture of Gaussians (MoG) with K_j components. Usually, pixel intensities at different sites can be assumed mutually independent given their labels, resulting in the distribution:

$$p(s_j(r)|z_j(r) = k) = \mathcal{N}(\mu_{jk}, \sigma_{jk}^2) \quad (2)$$

and

$$\begin{aligned} p(\mathbf{s}_j|\mathbf{z}_j) &= \prod_{r \in \mathcal{R}} p(s_j(r)|z_j(r)) \\ &= \prod_{r \in \mathcal{R}} \mathcal{N}(\mu_{jz_j(r)}, \sigma_{jz_j(r)}^2) \end{aligned}$$

where μ_{jk} and σ_{jk}^2 are the mean and variance of the k th Gaussian component of the j th source, and for $z_j(r) = k$, $\mu_{jz_j(r)} = \mu_{jk}$, $\sigma_{jz_j(r)}^2 = \sigma_{jk}^2$.

To more closely model the smoothness inside an image patch, that is, suppressing intensity variances brought by the i.i.d assumption (2), we introduce another layer of Markovian correlation between neighboring pixels directly on the intensities (illustrated as the gray links on the higher layer in Fig.1), as formulated below:

$$p(s_j(r)|z_j(r) = k, s_j(r'), r' \in \mathcal{V}(r)) = \mathcal{N}(\hat{\mu}_j(r), \hat{\sigma}_j^2(r)) \quad (3)$$

with,

$$\begin{aligned} \hat{\mu}_j(r) &= (1 - q_j(r))\bar{\mu}_j(r) + q_j(r)\mu_{jk} \\ \hat{\sigma}_j^2(r) &= (1 - q_j(r))\bar{\sigma}_j^2(r) + q_j(r)\sigma_{jk}^2 \end{aligned}$$

where, $q_j(r)$ is a binary valued contour computed from the label field:

$$q_j(r) = \begin{cases} 0 & \text{if } \mathbf{z}_j(r') = \mathbf{z}_j(r), \forall r' \in \mathcal{V}(r) \\ 1 & \text{else} \end{cases}$$

Based on the regions delimited by the contours, local mean

$$\bar{\mu}_j(r) = \frac{1}{|\mathcal{V}_{jk}(r)|} \sum_{r' \in \mathcal{V}_{jk}(r)} s_j(r')$$

where $\mathcal{V}_{jk}(r)$ denotes the intersection of the neighbor sites $\mathcal{V}(r)$ with the class k site set $\mathcal{R}_{jk} = \{r : \mathbf{z}_j(r) = k\}$. $\bar{\sigma}_j^2(r)$ is the *a priori* variance of pixel values inside a region.

From (3), we can see that the Markovian on intensity is conditionally activated based on whether the pixel is inside a patch or on its border. For an inner pixel ($q_j(r) = 0$), the mean of its distribution is determined by the average of its neighbours; For a contour pixel ($q_j(r) = 1$), it has the class distribution parameters just as the i.i.d case (2).

3 The BSS model

The BSS characteristic of the problem this paper addresses introduces another layer of probabilistic causality on top of the HMRF model described in former section, as shown in Fig.2, making it different from usual restoration or segmentation tasks. Here, what we observed are M images $(\mathbf{x}_i)_{i=1 \dots M}$, either monochromatic or multichromatic, considered to be generated by mixing N independent source

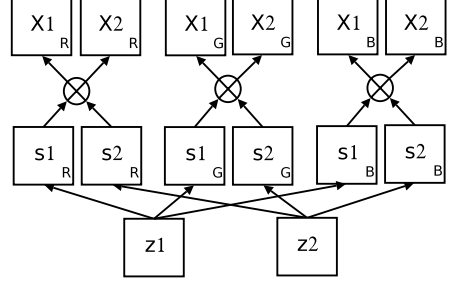


Figure 2. The BSS generation model on HMRF (with two sources and two observed mixtures in RGB channels).

images $(\mathbf{s}_j)_{j=1 \dots N}$ ($M \geq N$) with unknown mixing coefficients, which are additional latent variables to be estimated besides source image intensities and labels.

In this work, we concentrate on the linear instantaneous mixing model:

$$\mathbf{x}(r) = \mathbf{A}\mathbf{s}(r) + \epsilon(r) \quad r \in \mathcal{R} \quad (4)$$

where $\mathbf{x}(r) = [\mathbf{x}_1(r) \dots \mathbf{x}_M(r)]^t$, $\mathbf{s}(r) = [\mathbf{s}_1(r) \dots \mathbf{s}_N(r)]^t$, $\mathbf{A} = (a_{ij})_{M \times N}$ is the unknown mixing matrix, $\epsilon(r)$ is a set of independent zero-mean white Gaussian noise for each observation with variance $(\sigma_{\epsilon_i}^2)_{i=1 \dots M}$.

Let $\mathbf{S} = \{\mathbf{s}(r), r \in \mathcal{R}\}$, $\mathbf{X} = \{\mathbf{x}(r), r \in \mathcal{R}\}$, and denote the noise covariance matrix by $\mathbf{R}_\epsilon = \text{diag}(\sigma_{\epsilon_1}^2 \dots \sigma_{\epsilon_M}^2)$. With the assumption that mixing at different sites are mutually independent, we have the Gaussian distribution for the observations given the sources and the mixing parameters:

$$p(\mathbf{X}|\mathbf{S}, \mathbf{A}, \mathbf{R}_\epsilon) = \prod_r \mathcal{N}(\mathbf{A}\mathbf{s}(r), \mathbf{R}_\epsilon) \quad (5)$$

As illustrated by Fig.2, the separate labeling layer in the proposed HMRF model, which is different from the flat image model in [8], brings much flexibility in handling multichromatic color images. Usually, the availability of extra color channels help to acquire consistent labeling and stable clustering of homogeneous patches, which is critical for proper separation. To account for various mixing forms of multi-channel images, the mixing matrix \mathbf{A} can be generalized to a block matrix $[\mathbf{A}_{ij}]_{ML \times NL}$ (supposing L color channels), in which submatrices correspond to mixings in or between different channels. Taking the RGB representation for example (supposing two sources and observations),

$$\mathbf{A} = \begin{bmatrix} \mathbf{A}_R & \dots & \dots \\ \vdots & \mathbf{A}_G & \vdots \\ \dots & \dots & \mathbf{A}_B \end{bmatrix}_{6 \times 6}$$

In this paper, we adopt the mixing model following Fig.2, where the mixing occurs independently in each channel, so that \mathbf{A} is block diagonal with different main diagonal submatrices. Furthermore, only one label field \mathbf{z}_j is maintained for each multichromatic source $\mathbf{s}_j^{(R,G,B)}$, which enforces a common segmentation of pixels among different channels and is supposed to give more stable segmentation through this extra layer of correlation. The label field is then serially updated during the iterative estimation of each of $\mathbf{A}_{\{R,G,B\}}$, as described below.

4 Model parameter estimation

The unknown variables we want to estimate in the model given above are $\{\mathbf{S}, \mathbf{Z}, \mathbf{A}\}$ and hyperparameters of relevant distributions. The Bayesian estimation approach consists of deriving the posterior distribution of all the unknowns given the observation and adopting appropriate estimators such as the *maximum a posteriori* (MAP) or the *posterior mean* (PM) based on the posterior distribution. With our model assumptions, the joint *a posteriori* distribution of all unknown variables can be expressed as:

$$p(\mathbf{S}, \mathbf{Z}, \Theta | \mathbf{X}) \propto p(\mathbf{X} | \mathbf{S}, \mathbf{A}, \mathbf{R}_\epsilon) p(\mathbf{S} | \mathbf{Z}, \Theta_s) p(\mathbf{Z}) p(\Theta) \quad (6)$$

where, $\Theta_s = \{(\mu_{jk}, \sigma_{jk}^2), j = 1 \dots N, k = 1 \dots K\}$ and $\Theta = \{\mathbf{A}, \mathbf{R}_\epsilon, \Theta_s\}$.

Given (6), we compute the posterior mean estimation of unknown parameters by the MCMC Gibbs sampling algorithm, based on the full-conditional posterior distributions corresponding to each parameter in question, fixing all the others to their current values.

The Algorithm

- 1) Initialize $\mathbf{A}^{(0)}$, $\mathbf{S}^{(0)}$, $\mathbf{Z}^{(0)}$ and $\{\mu_{jk}, \sigma_{jk}^2\}$, either randomly or by *K-mean* clustering.
- 2) Repeat until converge,

- Simulating $\mathbf{S}' \sim p(\mathbf{S} | \mathbf{X}, \mathbf{Z}, \Theta)$:

$$\begin{aligned} p(\mathbf{S} | \mathbf{X}, \mathbf{Z}, \Theta) &\propto p(\mathbf{X} | \mathbf{S}, \mathbf{A}, \mathbf{R}_\epsilon) p(\mathbf{S} | \mathbf{Z}, \Theta_s) \\ &= \prod_r \mathcal{N}(\mathbf{m}_s^{apost}(r), \mathbf{R}_s^{apost}(r)) \end{aligned}$$

where,

$$\begin{aligned} \mathbf{R}_s^{apost}(r) &= [\mathbf{A}^t \mathbf{R}_\epsilon^{-1} \mathbf{A} + \Sigma_{\mathbf{z}(r)}^{-1}]^{-1} \\ \mathbf{m}_s^{apost}(r) &= \mathbf{R}_s^{apost}(r) [\mathbf{A}^t \mathbf{R}_\epsilon^{-1} \mathbf{x}(r) + \Sigma_{\mathbf{z}(r)}^{-1} \mathbf{m}_{\mathbf{z}(r)}] \end{aligned}$$

and, $\mathbf{m}_{\mathbf{z}(r)} = [\mu_{1z_1(r)}, \dots, \mu_{Nz_N(r)}]^t$ and $\Sigma_{\mathbf{z}(r)} = \text{diag}[\sigma_{1z_1(r)}^2, \dots, \sigma_{Nz_N(r)}^2]$.

- Simulating $\mathbf{Z}' \sim p(\mathbf{Z} | \mathbf{S}', \mathbf{X}, \Theta)$:

$$p(\mathbf{Z} | \mathbf{S}, \mathbf{X}, \Theta) \propto p(\mathbf{X} | \mathbf{Z}, \Theta) p(\mathbf{Z}) \quad (7)$$

and,

$$\begin{aligned} p(\mathbf{X} | \mathbf{Z}, \Theta) &= \prod_r p(\mathbf{x}(r) | \mathbf{z}(r), \Theta) \\ &= \prod_r \mathcal{N}(\mathbf{A} \mathbf{m}_{\mathbf{z}(r)}, \mathbf{A} \Sigma_{\mathbf{z}(r)} \mathbf{A}^t + \mathbf{R}_\epsilon) \end{aligned}$$

and, $p(\mathbf{Z}) = \prod_{j=1}^N p(\mathbf{z}_j)$, $p(\mathbf{z}_j)$ is Potts-MRF as (1), which is simulated by an inner Gibbs sampling.

- Simulating $\Theta = (\mu_{jk}, \sigma_{jk}^2, \mathbf{R}_\epsilon, \mathbf{A})$:
For computation simplicity, conjugate priors are chosen for respective hyperparameters:

- Gaussian for source means μ_{jk} ,
- Inverse Gamma for source variances σ_{jk}^2 ,
- Gaussian or uniform for mixing coefficients \mathbf{A}_{ij} ,
- Inverse Gamma for variances of mutually independent mixing noises $\sigma_{\epsilon i}^2$ (diagonal \mathbf{R}_ϵ).

Details about conjugate prior selection for hyperparameters and corresponding posterior derivation are omitted here for brevity, one can refer to [7] for more detailed discussion.

- 3) Based on the samples generated in iterations (skipping those from initial burn-in runs), compute the sample mean as the PM estimations for unknown parameters.

The Mean Field Approximation

The computation concerning the distribution of a MRF, like the prior $p(\mathbf{Z})$ and consequently the conditional posterior $p(\mathbf{Z} | \mathbf{X}, \mathbf{S}, \Theta)$ in (7), is usually intractable since the unfactorizable interactions of sites. To reduce the computation cost, the *mean field* approximation (MFA) [9], a special instance of variational methods effective for MRF, can be exploited to give a separable approximation in site r to the concerned joint distribution:

$$p(\mathbf{z}) \approx q(\mathbf{z}) \propto \prod_r q(\mathbf{z}(r) | \bar{\mathbf{z}}(r'), r' \in \mathcal{V}(r))$$

where $\bar{\mathbf{z}}(r')$ is the expected value of $\mathbf{z}(r')$ computed iteratively using $q(\mathbf{z})$. Now, (7) is approximated by

$$\begin{aligned} q(\mathbf{Z} | \mathbf{X}, \Theta) &= \prod_r q(\mathbf{z}(r) | \bar{\mathbf{z}}(r'), r' \in \mathcal{V}(r), \mathbf{x}(r), \Theta) \\ &= \prod_r p(\mathbf{x}(r) | \mathbf{z}(r), \Theta) q(\mathbf{z}(r) | \bar{\mathbf{z}}(r'), r' \in \mathcal{V}(r)) \end{aligned}$$

where, the expected value $\bar{z}(r)$ with respect to \mathbf{z} 's posterior $q(\mathbf{z}(r)|\cdot)$ can be computed iteratively by:

$$\bar{z}(r) = \frac{\sum_{\mathbf{z}(r)} \mathbf{z}(r) q(\mathbf{z}(r)|\bar{\mathbf{z}}(r'), \mathbf{x}(r), \Theta)}{\sum_{\mathbf{z}(r)} q(\mathbf{z}(r)|\bar{\mathbf{z}}(r'), \mathbf{x}(r), \Theta)}$$

Actually, if we perform optimization in place of simulation in our Gibbs sampling algorithm, we get EM or ICM alike algorithm for all hidden variables, where the mean field approximation allows the efficient calculation of involved conditional expectations over $p(\mathbf{z}|\mathbf{x}, \Theta)$.

Computational considerations

Aside from the mean field approximation, the posterior simulation of the individual labels $\{\mathbf{z}(r), r \in \mathcal{R}\}$ and intensities $\{\mathbf{s}(r), r \in \mathcal{R}\}$ (given values on other sites and of other variables) can be implemented in a parallel manner as a result of the choice of the first order neighborhood system (4 nearest neighbors) for both the intensity field \mathbf{s} and the label field \mathbf{z} . We divide the whole set of sites \mathcal{R} into two separate and interleaved subsets - \mathcal{R}_B and \mathcal{R}_W like the chessboard. Notice that $p(\mathbf{z}_B|\mathbf{z}) = p(\mathbf{z}_B|\mathbf{z}_W)$ and $p(\mathbf{z}_B|\mathbf{z}_W)$ is separable by site r , the same property applies to $p(\mathbf{z}_W|\mathbf{z}_B)$, $p(\mathbf{s}_B|\mathbf{s}_W, \mathbf{z})$ and $p(\mathbf{s}_W|\mathbf{s}_B, \mathbf{z})$. Therefore, the simulation of \mathbf{z} and \mathbf{s} , in each iteration, can now be performed parallelly for all sites of \mathcal{R}_B in one step and those of \mathcal{R}_W in the next step with much higher efficiency.

5 Experiments

To evaluate the performance of the proposed separation model, we test it on both synthetic and real world image mixtures. The synthetic images were simulated from a known generation model in three steps:

- i) Two label images $\mathbf{z}_{j=1,2}$ were generated according to the Potts-Markov prior model (1) with $\beta = 2$, with preselected class numbers $K_{j=1,2}$;
- ii) Two source images $\mathbf{s}_{j=1,2}$ were generated based on corresponding label fields according to (2), with randomly chosen mean and variance of pixel values for each class (Gaussian component) of each source;
- iii) Two mixture images $\mathbf{x}_{j=1,2}$ were generated according to (4) by linearly mixing two source images with a random chosen matrix $\mathbf{A}_{2 \times 2}$ and finally the white Gaussian noises \mathbf{R}_ϵ were added.

To quantitatively measure the separation performance, a normalized square error (NSE) is defined for each couple of original (\mathbf{s}_0) and estimated ($\bar{\mathbf{s}}$) sources.

$$\text{NSE}(\bar{\mathbf{s}}, \mathbf{s}_0) = \sqrt{\sum_r (\bar{\mathbf{s}}(r) - \mathbf{s}_0(r))^2 / \sum_r \mathbf{s}_0(r)^2}$$

Fig.3 shows the separation result on two synthetic samples with $K = 2, 3$ respectively. Table 1 shows the posterior mean estimation for the mean of each Gaussian component of the source distribution.

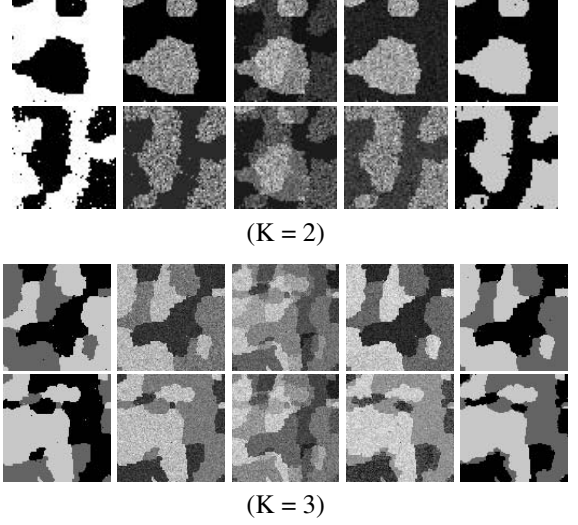


Figure 3. Separation of synthetic image mixtures (columns from left to right are: ground-truth labels, synthetic sources, noisy mixtures, demixed sources, estimated labels).

Table 1. Comparison of the estimated ($\bar{\mu}$) and the original (μ_0) mean of each label component of two sources (1)(2) in Fig.3.

	K = 2		K = 3		
$\mu_0^{(1)}$	0.2	0.7	0.2	0.4	0.8
$\bar{\mu}^{(1)}$	0.2249	0.6402	0.1554	0.3933	0.7971
$\mu_0^{(2)}$	0.3	0.6	0.3	0.5	0.8
$\bar{\mu}^{(2)}$	0.2713	0.5864	0.2877	0.5037	0.8019
NSE	0.0114		0.0275		

For comparison, we applied the FastICA algorithm [4] on the sample images, using its default parameter set. The output independent components are shown in Fig.4, which approach the original sources pretty well, since the close match of the data generation model with ICA assumption.

For real world image samples, we chose the mixed text images resulting from the showing-through effect, which often occurs in the digitization of duplex printed documents. Due to the non-opaque medium, the backside text appear and get mixed in the scanned image with the foreside text. We assume the mixing is linear and all foreground text of one side are approximately same colored, hence we can nat-

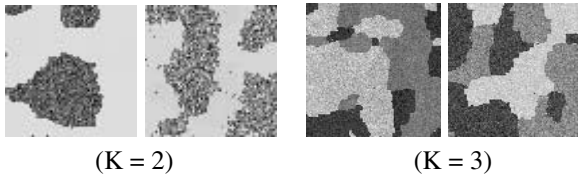


Figure 4. Separation results by ICA on synthetic images in Fig.3.

usually fix $K = 2$ (background and text). With the proposed two-layer MRF model (3) of sources, the separation result is shown in Fig.5.

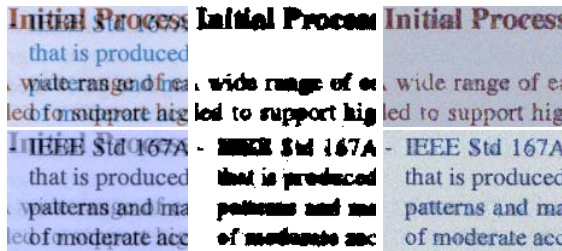


Figure 5. Separation of real showing-through mixtures of text patterns (columns from left to right are: mixtures, estimated labels, demixed sources).

Fig.6 shows the separation result by FastICA on the real images. Since no explicit treatment for multi-channel data specified in ICA, all three channels (RGB) of the two mixtures were fed to the algorithm. The demixed sources were found in two of six independent components outputted. Due to the unignorable noises, however, the vanilla ICA algorithm sometimes could not give complete separation of the sources as shown by Fig.6. As the mixing noises and correlations of sources became comparatively significant, we noticed in some experiments that ICA could separate noises from the mixed signals instead of demixing real sources. Comparatively, for large part of these cases the proposed model usually exhibits favorable stability as a result of the consistency enforced by HMRF.

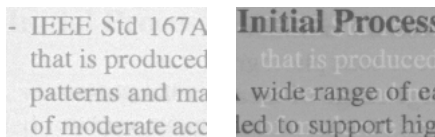


Figure 6. Separation results by ICA on real image samples in Fig.5.

6 Conclusions

We presented a Bayesian framework for blind separation of multichromatic image mixtures. An hierarchical Markov random field model is proposed to enforce both the consistent segmentation among all channels of one source image and the piecewise homogeneity on different layers of interacting image elements - the labels and intensities. Based on this HMRF model, we consider the classic BSS problem of separating noisy linear instantaneous mixtures of images. For all unknown variables, including the sources, the mixing matrix and relevant hyperparameters, we derive their posterior distributions and compute the posterior mean estimation by MCMC simulations. To reduce the computation demand associated with the MRF graphical model, approximation based on mean field theory is also considered. Favorable results were obtained in experiments on both synthetic and real world images.

Acknowledgements

Research supported by the National Science Foundation of China under Grant Nos. 60721002.

References

- [1] L. B. Almeida. Separating a real-life nonlinear image mixture. *Journal of Machine Learning Research*, 6:1199–1232, 2005.
- [2] A. M. Bronstein, M. M. Bronstein, M. Zibulevsky, and Y. Y. Zeevi. Sparse ICA for blind separation of transmitted and reflected images. *Intl. Journal of Imaging Science and Technology (IJIST)*, 15:84–91, 2005.
- [3] V. D. Calhoun and T. Adali. Unmixing fMRI with independent component analysis. *IEEE Engineering in Medicine and Biology Magazine*, 25(2):79–90, Mar. 2006.
- [4] A. Hyvarinen. Fast and robust fixed-point algorithms for independent component analysis. *IEEE Transactions on Neural Networks*, 10(3):626–634, 1999.
- [5] A. Hyvarinen, J. Karhunen, and E. Oja. *Independent Component Analysis*. John Wiley & Sons, Inc., New York, 2001.
- [6] L. Parra, C. Spence, A. Ziehe, K.-R. Muller, and P. Sajda. Unmixing hyperspectral data. In *Advances in Neural Information Processing Systems*, volume 12, pages 942–948, 2000.
- [7] H. Snoussi and A. Mohammad-Djafari. Fast joint separation and segmentation of mixed images. *Journal of Electronic Imaging*, 13:349–361, Apr. 2004.
- [8] A. Tonazzini, L. Bedini, and E. Salerno. A markov model for blind image separation by a mean-field EM algorithm. *IEEE Transactions on Image Processing*, 15(2):473–482, Feb. 2006.
- [9] J. Zhang. The mean field theory in EM procedures for blind markov random field image restoration. *IEEE Transactions on Image Processing*, 2(1):27–40, 1993.